Proc. NIPR Symp. Polar Meteorol. Glaciol., 5, 156–166, 1992

ANALYSIS OF MOS-1 MSR DATA RECEIVED AT SYOWA STATION, ANTARCTICA

Takashi YAMANOUCHI[1], Tomoyuki OSHIYAMA[2]* and Makoto WADA[1]

[1]*National Institute of Polar Research, 9–10, Kaga 1-chome, Itabashi-ku, Tokyo 173*

[2]*University of Electro-Communications, 5–1, Chofugaoka 1-chome, Chofu-shi, Tokyo 182*

Abstract: Atmospheric parameters and ground surface information are obtained using the MOS-1 MSR data received at Syowa Station, Antarctica. Several difficulties have appeared in the process of deriving water vapor amount and liquid water content. One is the antenna temperature, which includes large bias error; this causes the largest uncertainty. Also, the antenna temperature near the coast of the Antarctic continent was greatly affected by high brightness temperature of the ice sheet owing to the antenna side lobe, which caused difficulties in comparing with ground-based observations as a validation. In the normal condition, for the present example, water vapor amount ranged from 0.4 to 1.4 g/cm^2 and liquid water content from 0 to 14 mg/cm^2. However, there was found a belt of high liquid water content in some paths, corresponding to a high brightness temperature of about 190 K. The atmospheric water vapor or liquid water affects the estimation of surface conditions such as sea ice concentration. It is difficult to obtain atmospheric parameters over the ice sheet and sea ice, on account of their high and variable brightness temperature.

1. Introduction

The data of Marine Observation Satellite (MOS)-1 have been received at Japanese Antarctic Station, Syowa (69°00′S, 39°35′E), since February 1989 with the installation of a new antenna system (Multi Purpose Satellite Data Receiving System), aiming to obtain parameters of the polar atmosphere and cryosphere (YAMANOUCHI *et al.*, 1991). From the Microwave Scanning Radiometer (MSR) data, it is planned to derive atmospheric water vapor and cloud liquid water content, sea ice condition, concentration and extent, and characteristics of the ice sheet surface. However, since microwave radiations of the frequencies adopted by MSR contain both effects of the atmosphere and the ground (surface), it is difficult to separate the two effects. It is necessary to develop an effective method to determine atmospheric parameters and ground surface properties independently.

In the present paper, several difficulties which appeared in the course of analyzing the newly acquired MSR data are described. The MSR data dealt with in the present paper are only for a few paths in February 1989, received at the beginning of the system operation. Since the present data include only a small amount of sea ice, discussion is

* Present address: Environmental Sciences, University of Tsukuba, 1–1, Tennodai 1-chome, Tsukuba 305.

concentrated on analysis of atmospheric water vapor and liquid water content. In 1989, data of more than 150 paths were acquired throughout the year, and analysis of sea ice shall be done in detail in the next paper.

2. Data and Analysis

The MOS-1 MSR consists of two sensors of 23.8 and 31.4 GHz, and is rotated around the satellite nadir axis with inclination of 10 degrees (conical scan). The outputs of these sensors are integrated during 10 or 47 ms for the respective frequencies and consist of 4 channels as shown in Table 1 (NASDA, 1985). Processing to level 2 was done at Earth Observation Center of National Space Development Agency of Japan (NASDA EOC); it included radiometric calibration and geometric conversion to the polar stereographic map projection imagery. In the course of geometric conversion, data were resampled to the gridded points. The sampling method in normal processing at NASDA EOC is "special resampling (SR)", which is a weighted mean of the data using the antenna pattern as a weighting function. Also, nearest neighbor resampling (NN) was done for the present data. Samplings were done 30 km apart on the 23.8 GHz channel and 20 km apart on the 31.4 GHz channel, respectively, and plotted on 10 km grid points. These sampling scales roughly coincide with the horizontal resolution—instantaneous field of view—of sensors, 32 and 23 km, respectively.

The microwave brightness temperature T_B, which is proportional to the radiance, measured from a satellite is expressed as follows using the ground surface temperature T_s, surface emissivity ε_s, transmittance of the atmosphere τ and atmospheric temperature $T(z)$ at height z,

$$T_B=\varepsilon_s T_s\tau+\int T(z)\frac{\partial\tau}{\partial z}dz+\tau(1-\varepsilon_s)\int T(z)\frac{\partial\tau}{\partial z}dz\ . \tag{1}$$

Table 1. Specifications of Microwave Scanning Radiometer (MSR) (NASDA, 1985).

Item	Characteristics	
Frequency (GHz)	23.8±0.2	31.4±0.25
(Wavelength, cm)	1.26	0.955
Beam width	1.89±0.19°	1.31±0.13°
(Field of view, km)	32	23
Integration time (ms)	10 and 47	10 and 47
Swath width	317 km	
Scan	Mechanical (conical scanning)	
Dynamic range	30–330 K	
Antenna	Offset Cassegrain type	
Receiver	Dicke type	
Polarization	Horizontal	Vertical
Radiometric resolution	1 K	
Scan period	3.2 s	
Quantization level	1024 (10 bits)	
Data rate	2 kbits/s	

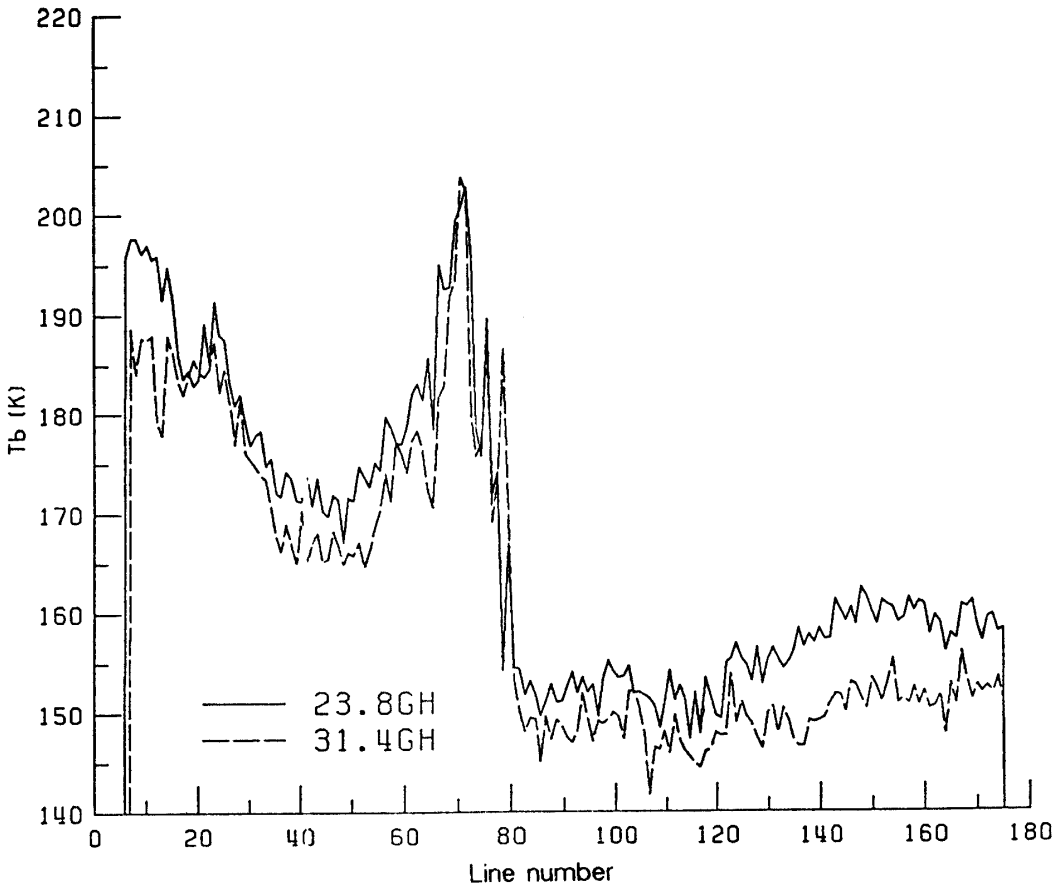

Fig. 1. Variation of brightness temperature of channel 1 (23.8 GHz, 10 ms) and 3 (31.4 GHz, 10 ms) of MSR along the orbit, path 69, February 15, 1989. Abscissa indicates line number (30 km each) from the data end.

The first term on the right hand side is emission from the surface transmitted through the atmosphere, the second term is upward atmospheric emission and the third term is downward atmospheric emission which is reflected at the surface and transmitted through the whole atmosphere. The surface information is available from the first term, when the second and third term and transmissivity τ work as a disturbance; while the second and third terms contribute to the retrieval of the atmospheric parameters, when the first term ε_s or T_s interrupts the result.

As a typical example, Fig. 1 shows one of the cross sections of MSR data along the satellite orbit, T_B of 23.8 (channel 1) and 31.4 (channel 3) GHz, of path 69, received on February 15, 1989. This is a descending path from the Southern Ocean to the Antarctic continent and ends around the Ronne Ice Shelf, as shown in Fig. 2. In Fig. 1, lines are numbered from the end of the path and left hand side to the line 70 for the ice sheet, where the brightness temperature ranges from about 170 to 200 K. High brightness temperature appears near the coast and then gradually decreases inland on account of low physical temperature and smaller emissivity of surface snow (COMISO *et al.*, 1982). The right hand side is for the ocean, where the brightness temperature ranges around 150 K, and varies about 10 K owing mainly to the variation

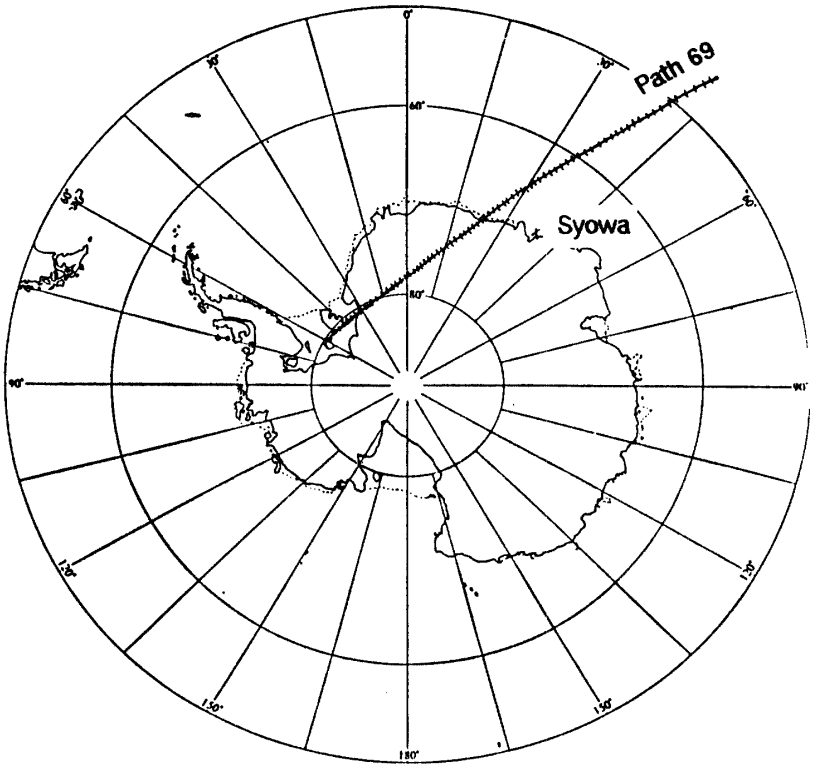

Fig. 2. Nadir points of MOS-1 path 69, of which data are shown in Fig. 1, received at Syowa Station on February 15, 1989.

of atmospheric water vapor and liquid water content, and also to the variation of sea surface condition. Since the data are in summer, sea ice exists in only a narrow region between line number 70 and 80; however, because of the large effect of the antenna side lobe, it is difficult to correlate the antenna temperature with the brightness temperature or the actual geophysical parameters, and to discuss in the narrow coastal region in detail.

3. Derivation of Liquid Water Content and Water Vapor Amount

Water vapor amount and liquid water content can be estimated from the brightness temperatures on 23.8 and 31.4 GHz. Since little sea ice exists in the data, we tried first to estimate atmospheric parameters. In the microwave region, an absorption line of water vapor exists at 22.235 GHz. On the other hand, absorption coefficients of small water droplets increase gradually with frequency in this frequency region. Thus, it is possible to derive water vapor amount and liquid water content separately from the measurements at two frequencies near and far from the water vapor absorption line. This is a possible way to derive water vapor amount and liquid water content; however, as seen in eq. (1), since the transmissivity of the total atmosphere τ does not drop to 0, the surface term is still affecting the brightness temperature. We have to postulate some realistic hypothesis. If we define an equivalent temperature of the atmosphere T_a as

$$T_a(1-\tau)=\int T(z)\frac{\partial \tau}{\partial z}\,dz\,, \tag{2}$$

then eq. (1) will be written as

$$\begin{aligned} T_B&=\varepsilon_s T_s\tau+T_a(1-\tau)+(1-\varepsilon_s)T_a\tau(1-\tau)\\ &=\varepsilon_s T_s+[T_a-\varepsilon_s T_s+(1-\varepsilon_s)T_a\tau](1-\tau)\,. \end{aligned} \tag{3}$$

If we assume $T_a=T_s$,

$$T_B=\varepsilon_s T_s+(1-\varepsilon_s)T_s(1-\tau^2)\,. \tag{4}$$

Since the atmospheric transmissivity $\tau=\exp(-\gamma)$ is nearly equal to 1, eq. (4) can be approximated as

$$\gamma=\frac{1}{2T_s(1-\varepsilon_s)}T_B-\frac{\varepsilon_s}{2(1-\varepsilon_s)}\,. \tag{5}$$

γ is composed of three components, water vapor $\gamma(H_2O)$, oxygen $\gamma(O_2)$ and liquid water $\gamma(LW)$, as:

$$\gamma=\gamma(H_2O)+\gamma(LW)+\gamma(O_2)\,. \tag{6}$$

$\gamma(H_2O)$ and $\gamma(O_2)$ were estimated from the calculation of a simple model atmosphere, assuming typical Antarctic temperature and water vapor profiles (summer and winter means at Syowa Station), using the absorption coefficient proposed by KREISS (1968) for each sub-layer. From the obtained transmissivities of the total atmospheric layer, $\gamma(H_2O)$ was approximated by the linear relation to the column water vapor amount V as

$$\gamma(H_2O)=\alpha\cdot V\,, \tag{7}$$

and the mean value of $\gamma(O_2)$ was decided. Absorption coefficient β for the liquid water content W was derived from the results by STAELIN *et al.* (1976) as

$$\beta=1.11\cdot 10^{0.0122(291-T)-3}\cdot\nu^2\,, \tag{8}$$

where ν is a microwave frequency (GHz) and T (K) is temperature. Obtained values of α, β and $\gamma(O_2)$ are listed in Table 2. Then eq. (5) can be rewritten in the linear equation for V and W as

$$\alpha V+\beta W+\gamma(O_2)=aT_B+b\,, \tag{9}$$

where aT_B and b are the first and second terms of the right-hand side of eq. (5).

Table 2. Absorption coefficients α for water vapor, β for liquid water and optical depth of oxygene $\gamma(O_2)$.

	α ($g^{-1}\,cm^2$)	β ($g^{-1}\,cm^2$)	$\gamma(O_2)$
23.8 GHz	0.05	1.83	0.006
31.4 GHz	0.02	3.18	0.015

Equation (9) is applied to both 23.8 and 31.4 GHz, and V and W can be solved from the system of equations using the brightness temperatures on both channels. Before solving the equations, we have to calculate a and b from surface parameters ε_s and T_s, which have to be measured. However, since we do not have direct measurements of ε_s and T_s, typical mean values for the southern ocean near 273 K are used as T_s, and 0.46 and 0.49 as ε_s for 23.8 and 31.4 GHz, respectively.

The data of path 69, whose cross section is shown in Fig. 1, were used as a typical example for the analysis of water vapor amount and liquid water content. Before calculating the results, we have to determine bias error. The lowest value is estimated for a clear sky with 0 mg/cm^2 of liquid water and 0.5 g/cm^2 of water vapor, which results in $T_{23}=135$ K and $T_{31}=141$ K from eq. (9). However, the actual lowest values seen in Fig. 1 are much higher than these values, especially for T_{23}. We call these differences the "bias errors", 12 and 0.2 K for T_{23} and T_{31}, respectively. These numbers are in good accordance with the summations of "antenna pattern correction" and "bias correction" obtained by SHIBATA *et al.* (1990). After subtracting the present "bias errors", water vapor amount V and liquid water content W are derived from eq. (9). Figure 3 shows the results corresponding to the brightness temperature shown in Fig. 1, only for those over the ocean. In these results, water vapor varies from 0.4 to 1.4 g/cm^2, with mean value of 0.84 g/cm^2, 0.6 g/cm^2 near the continent and increases toward lower latitude to about 1.2 g/cm^2 north of 60°S. Liquid water content

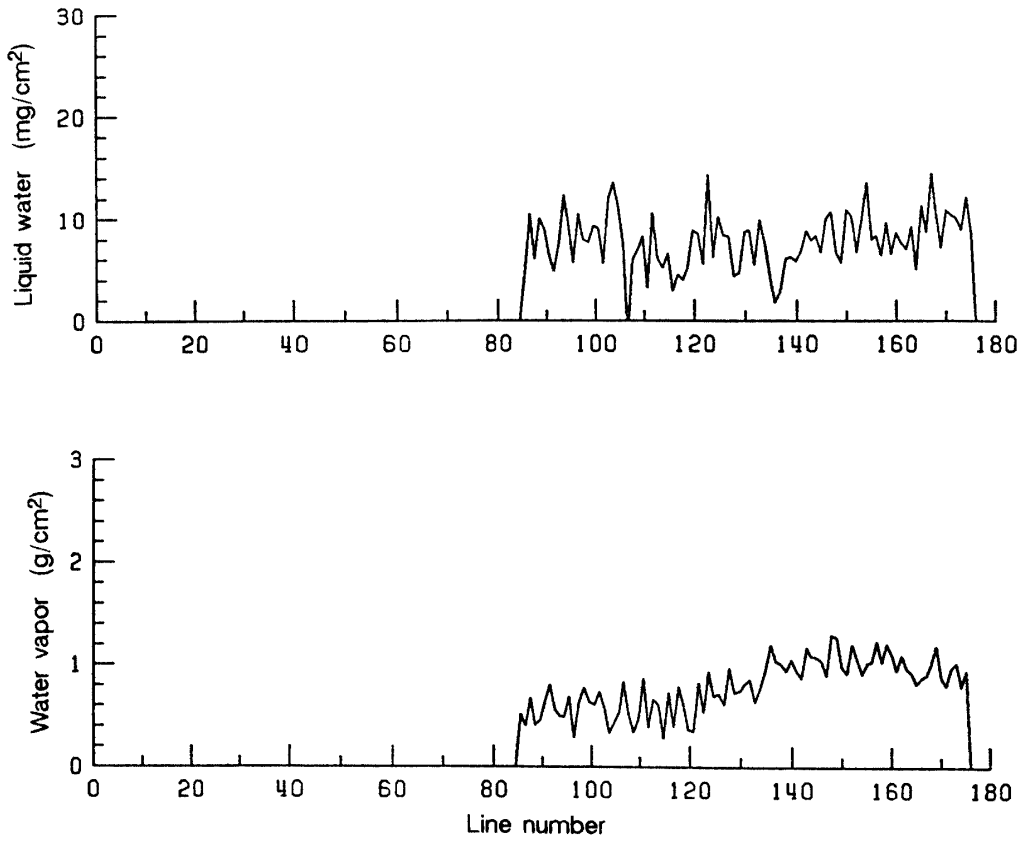

Fig. 3. Liquid water content and water vapor amount obtained from the brightness temperature of Fig. 1, along the orbit, path 69, February 15, 1989.

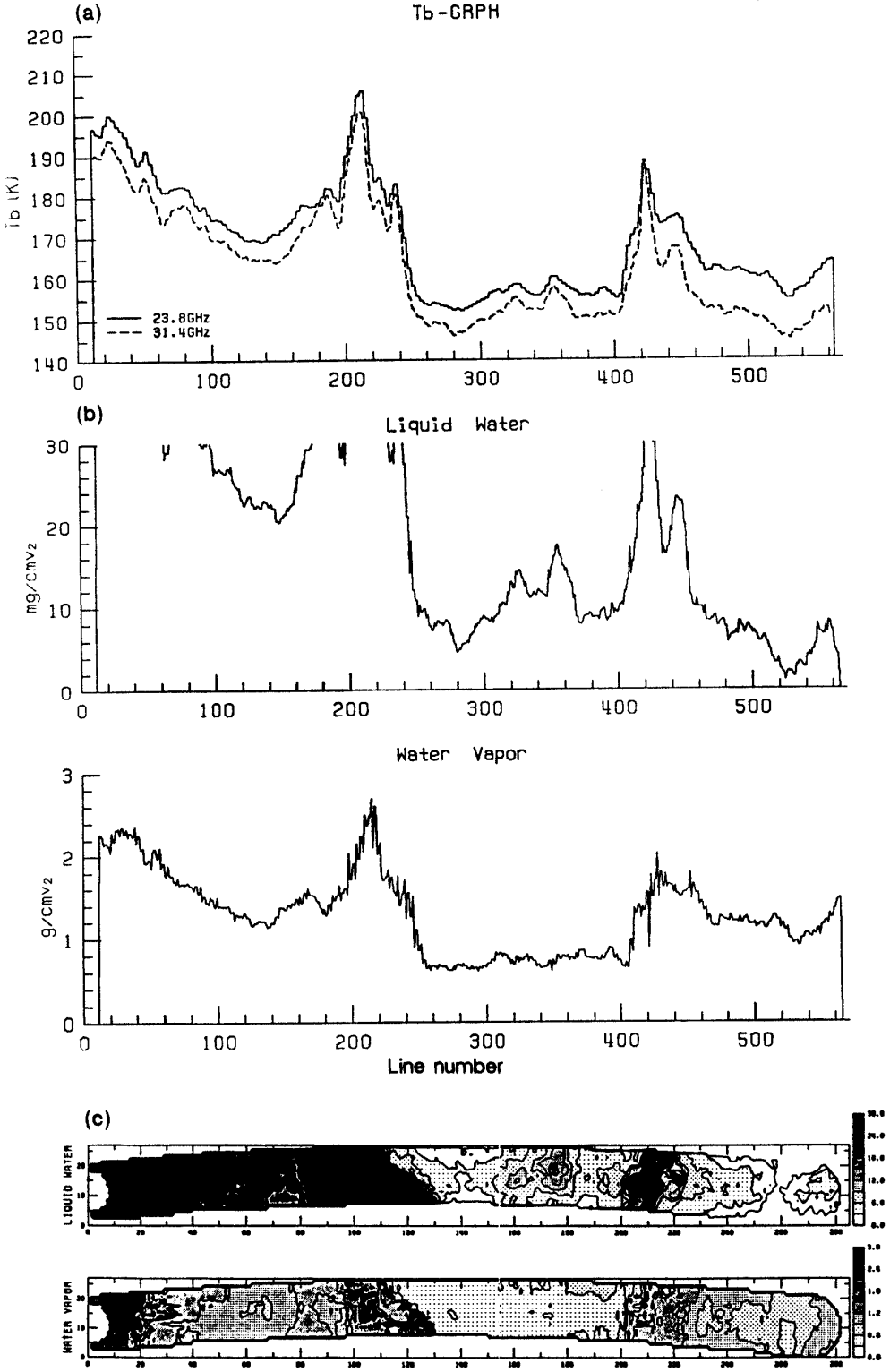

Fig. 4. *(a) Brightness temperature of channel 1 and 3 of MSR along the orbit, path 67, February 13, 1989. Abscissa indicates line number (10 km each) from the data end. (b) Liquid water content and water vapor amount correspond to (a). (c) Horizontal distribution of liquid water content and water vapor amount from MSR path 67. For (b) and (c), results are meaningless until about line 240.*

ranges between 0 to 14 mg/cm^2, and is about 7.2 mg/cm^2 on average.

Water vapor amount and liquid water content are also obtained from another data set of path 67, February 13, 1989. Brightness temperature as shown in Fig. 4 has large variation over ocean compared to Fig. 1. High frequency variations seen in Fig. 1 are smoothed out in this figure, because the data were obtained by special resampling (SR) explained in Section 2, whlie the data in Fig. 1 are of nearest neighbor sampling (NN) and have not passed any process of averaging. Apart from the data over the continent, brightness temperature of about 190 K appeared also over the ocean around line number 420, not owing to the sea ice or other surface condition, and attributable to the atmospheric effect, by comparing to the corresponding VTIR image. As seen in Fig. 4, large liquid water content, more than 30 mg/cm^2, and high water vapor amount are the results. Results are meaningless until line number 240 over the continent in (b) and (c). The results are also shown in horizontal distribution as in Fig. 4, indicating clearly the belt of high liquid water content over the ocean which corresponds to the dense cloud belt seen in the VTIR data.

4. Problems and Measures

It is needed to estimate the validity of the water vapor amount and liquid water content obtained in the previous section. As one method, several kinds of ground based observations using microwave radiometer, vertical pointing radar and PPI radar were made together with regular aerological and surface meteorological observations (WADA, 1990). However, MSR data to be compared with the ground based data obtained at Syowa Station are greatly affected by the contribution of the antenna side lobe, since the area is near the coast. The large difference in the brightness temperature between the sea surface and continental snow affects those values greatly. The effect of the antenna side lobe has been estimated theoretically (SUZUKI *et al.*, 1990) and empirically (OJIMA *et al.*, 1989; SHIBATA *et al.*, 1990) only for the case between land and ocean; we should establish a new relation for the case between ice sheet or sea ice and the ocean.

Over the continental ice sheet or sea ice, it is difficult to derive atmospheric parameters such as water vapor and liquid water content. It was possible to derive atmospheric parameters over open water, since the brightness temperature, or emissivity, of the sea surface is small ($\varepsilon_s \approx 0.5$) and does not show a large variation. However, if the emissivity and brightness temperature is large ($T_B \approx 200 \sim 230$ K), then it is difficult to derive atmospheric parameters precisely. In eq. (4), the second term ΔT_B

$$\Delta T_B = (1-\varepsilon_s) T_s (1-\tau^2) , \tag{10}$$

is attributed as an atmospheric effect. When ε_s becomes large, ΔT_B will be small and the atmospheric contribution on T_B will become small. In case of 0.5 g/cm^2 water vapor amount and 10 mg/cm^2 liquid water content, as seen, for example, in the polar atmosphere, ΔT_B is estimated as 2.5 and 2.9 K for 23.8 and 31.4 GHz, respectively, assuming $T_s = 253$ K. This small amount of atmospheric contribution will result in a large error for estimating water vapor and cloud liquid water content.

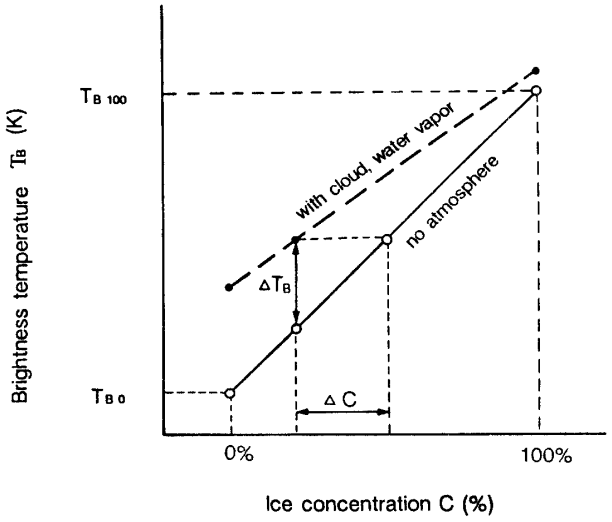

Fig. 5. Relation of sea ice concentration and microwave brightness temperature, and contribution of the atmospheric effect.

On the contrary, the atmospheric contribution will disturb the analysis of surface parameters. In case of negligible atmospheric effect, the surface parameters can be derived from the first term of the right hand side of eq. (4). However, the atmospheric contribution, if large, will cause large error in the brightness temperature, T_B, in obtaining $\varepsilon_s T_s$, especially when ε_s is small. It is found in Fig. 4 that the atmospheric components can become as great as 40 degrees in some cases (around line 420). These situation arise in the analysis of sea ice concentration, as schematically explained in Fig. 5.

Sea ice concentration can be obtained assuming a linear relation between brightness temperature and ice concentration (ZWALLY and GLOERSEN, 1977). This relation is shown by the solid line in Fig. 5 without any atmospheric contribution. The difference in ice concentration between 0 and 100% causes the difference in the surface brightness temperature between T_{B0} and T_{B100}. The difference found in the MSR data of September 1989 containing wide sea ice was about 80 K in this frequency range. The atmospheric effect ΔT_B will result in an error of ice concentration ΔC (broken line). The largest contribution of the atmosphere, about 40 K as explained in the last paragraph, when the concentration is low (low surface brightness temperature), can cause up to 50% error in the ice concentration analysis. When the concentration is large (large surface brightness temperature), $(1-\varepsilon_s)$ makes the atmospheric effect small and the error in the ice concentration small. ΔT_B of 2.5 and 2.9 K, for example, as already described, will amount to only 3 to 4% error of ice concentration analysis.

This complicated situation is owing partly to the frequency selection. 23.8 and 31.4 GHz is not a suitable pair for finding the surface parameters, and also 23.8 GHz is not optimal for sensing water vapor in the polar regions, since the water vapor amount is extremely small. The absorption of water vapor at this frequency is not strong enough. The sensing of the surface parameters might be much easier at a longer wavelength such as 10 or 18 GHz, and sensing of water vapor at 22 GHz and the

higher frequency channel for different information on the surface, adopted by Nimbus 7 SMMR (COMISO *et al.*, 1984).

In order to eliminate the error of sea ice concentration due to the atmospheric effect, especially cloud liquid water content, cloud information should be derived from data of other sensors such as the VTIR. The split window channel of the VTIR, channel 3 (11 μm) and channel 4 (12 μm) will provide some information on clouds by a method similar to that used by NOAA AVHRR (YAMANOUCHI *et al.*, 1987). However, the result may be not quantitative but only qualitative.

The atmospheric parameters obtained from MSR can be validated, if we can estimate and correct the side lobe effect of the MSR antenna. The validation can also be made by comparing the results by MSR for points far from the coast to the water vapor amount derived by NOAA HIRS/2 or to the optical depth or other parameters of clouds determined by NOAA AVHRR (ARKING and CHILDS, 1985; YAMANOUCHI *et al.*, 1987; YAMANOUCHI and KAWAGUCHI, 1992).

Derivations of sea ice information and concentrations from MSR data are subjects to be deal with in the near future.

Acknowledgments

The authors are grateful to the members of the 30th Japanese Antarctic Research Expedition led by Prof. M. EJIRI, National Institute of Polar Research, for receiving the MOS-1 data, especially to Mr. H. ARIYOSHI of NEC Corporation.

The MOS-1 data were processed by the Earth Observation Center of NASDA. The data were analyzed utilizing facilities of the Information Processing Center of the National Institute of Polar Research. This work was supported financially in part by a Grant-in-Aid for Scientific Research, No. 01646525 and 02228225, Ministry of Education, Science and Culture.

References

ARKING, A. and CHILDS, J. D. (1985): Retrieval of cloud cover parameters from multi spectral satellite images. J. Clim. Appl. Meteorol., **24**, 322–333.

COMISO, J. C., ZWALLY, H. J. and SABA, J. L. (1982): Radiative transfer modeling of microwave emission and dependence on firn properties. Ann. Glaciol., **3**, 54–58.

COMISO, J. C., ACKLEY, S. F. and GORDON, A. L. (1984): Antarctic sea ice microwave signatures and their correlation with *in situ* ice observations. J. Geophys. Res., **89**, 662–672.

KREISS, W. T. (1968): Meteorological observations with passive microwave systems. Boeing Scientific Research Laboratories Document, D1–82–0692, 198 p.

NASDA (NATIONAL SPACE DEVELOPMENT AGENCY OF JAPAN) (1985): MOS-1 to ground station interface discription. Rev. 1, HE-85317.

OJIMA, T., MAEDA, K. and SATOH, H. (1989): Investigation of atmospheric effect to MESSR, VTIR and MSR, and observations of oceanic phenomena using MSR. Proceedings of the Third Symposium on MOS-1 Verification Program (MVP). Tokyo, NASDA, 90–101.

SHIBATA, A., SHINOHARA, Y. and SHUTO, K. (1990): Investigations on verification of the data observed by the MESSR and VTIR, and on interannual trend in the MSR data. Proceedings of MOS-1 Data Evaluation, NASDA, March 1990. Tokyo, 52–63.

SUZUKI, T., ARAI, I. and MORITA, K. (1990): Signal processing of the data obtained by MOS-1 MSR. Proceedings of MOS-1 Data Evaluation, NASDA, March 1990. Tokyo, 71–91.

STAELIN, D. H., KUNZI, K. F., PETTYJOHN, R. L., POON, R. K. L. and WILCOX, R. W. (1976): Remote sensing of atmospheric water vapor and liquid water with the Nimbus-5 microwave spectrometer. J. Appl. Meteorol., **15**, 1204–1241.

WADA, M. (1990): Antarctic climate research data, Part 2. Radar and microwave radiometer data at Syowa Station, Antarctica from March to December 1988. JARE Data Rep., **153** (Meteorology 24), 97 p.

YAMANOUCHI, T. and KAWAGUCHI, S. (1992): Cloud distribution in the Antarctic from AVHRR and radiation measurements at the ground. Int. J. Remote Sensing, **13**, 111–127.

YAMANOUCHI, T., SUZUKI, K. and KAWAGUCHI, S. (1987): Detection of clouds in Antarctica from infrared multispectral data of AVHRR. J. Meteorol. Soc. Jpn., **65**, 949–962.

YAMANOUCHI, T., KANZAWA, H., ARIYOSHI, H. and EJIRI, M. (1991): Report on the first MOS-1 data received at Syowa Station, Antarctica. Proc. NIPR Symp. Polar Meteorol. Glaciol., **4**, 22–30.

ZWALLY, H. J. and GLOERSEN, P. (1977): Passive microwave images of the polar regions and research applications. Polar Rec., **18**, 431–450.

(Received January 10, 1991; Revised manuscript received May 1, 1991)